



## RESEARCH ARTICLE

### Isolation and Characterization of Fetal Adnexa-Derived Mesenchymal Stem Cells from Nili-Ravi Buffalo (*Bubalus bubalis*)

Adeel Sarfraz<sup>1</sup>, Anas Sarwar Qureshi<sup>1\*</sup>, Mansur Abdullah Sandhu<sup>2#</sup>, Rehmat Ullah Shahid<sup>1</sup> and Muhammad Naeem Faisal<sup>3</sup>

<sup>1</sup>Department of Anatomy, Faculty of Veterinary Science, University of Agriculture, Faisalabad, Pakistan

<sup>2</sup>Department of Veterinary Biomedical Sciences, Faculty of Veterinary and Animal Sciences, PMAS-Arid Agriculture University, Rawalpindi, Pakistan; <sup>3</sup>Institute of Physiology and Pharmacology, Faculty of Veterinary Science, University of Agriculture, Faisalabad, Pakistan

\*Corresponding author: [anas-sarwar@uaf.edu.pk](mailto:anas-sarwar@uaf.edu.pk); # Co-Corresponding author: [mansoorsandhu@uaar.edu.pk](mailto:mansoorsandhu@uaar.edu.pk)

#### ARTICLE HISTORY (21-047)

Received: January 23, 2021  
Revised: July 14, 2021  
Accepted: August 05, 2021  
Published online: September 02, 2021

#### Key words:

Amniotic fluid  
Mesenchymal stem cells  
Nili-Ravi buffalo  
Wharton's jelly

#### ABSTRACT

Mesenchymal stem cells (MSCs) are extremely valuable in veterinary and human medicine due to their potential application in regenerative medicine. The purpose of this study was to isolate, differentiate and characterize bovine MSCs (bMSCs) from fetal adnexa including amniotic fluid (AF) and Wharton's jelly (WJ) of Nili-Ravi buffalo during the second trimester. After slaughtering of the animals, pregnant uteri (n=3) were retrieved and properly disinfected before bMSC isolation. The cells from AF were isolated by centrifugation at 400g for 10 minutes, while from WJ by enzymatic digestion with trypsin-EDTA (0.05%). The isolated cells were studied for their plastic adherence, phenotype identification, metabolic activity and *in vitro* differentiation ability. The isolated AF and WJ bMSCs were fibroblast-like cells in their phenotype, adhered to plastic, showed similar metabolic potential and population doubling time (PDT), but proliferative activity was initially higher (P<0.05) in WJ-bMSCs. When appropriately induced, both cell types showed mesodermal differentiation into adipogenic and osteogenic lineages which was further affirmed by immunolocalization of fatty acid-binding protein 4 (FABP4) and osteopontin (OST), respectively. However, image analysis revealed that the osteogenic activity of WJ-bMSCs was significantly higher (P<0.05) than that of AF-bMSCs. MSC surface markers (CD73 and CD90) were also positively expressed by both cell types. The study showed that the fetal adnexa of buffalo is a rich source of MSCs for culture and has robust differentiation capabilities.

©2021 PVJ. All rights reserved

**To Cite This Article:** Sarfraz A, Qureshi AS, Sandhu MA, Shahid RU and Faisal MN, 2021. Isolation and characterization of fetal adnexa-derived mesenchymal stem cells from Nili-Ravi buffalo (*Bubalus bubalis*). Pak Vet J. <http://dx.doi.org/10.29261/pakvetj/2021.065>

#### INTRODUCTION

Over the past two decades, stem cell (SC) research is at the forefront of biological studies as these cells can regenerate, differentiate, and modulate the immune system; hence, they can be used in different therapeutic applications (de Moraes *et al.*, 2017). The most intensively studied SC are mesenchymal stem cells (MSCs) which can be obtained from fetal annexes by non-invasive protocols. Usually, these tissues are disposed of as medical waste otherwise. Unlike adult SCs (ASCs), these cells have better renewability and immunomodulatory properties (Kumar *et al.*, 2015; Campos *et al.*,

2017), which may be attributed to a close association with the fetus or late activation of senescent genes.

Amniotic fluid (AF) and Wharton's jelly (WJ) are commonly used fetal annexes for the isolation of MSCs. During pregnancy, AF acts as a shielding liquid around the fetus which is composed of secretions and excretions of the fetus and fetal membranes. It also contains factors for fetal growth and development as well as have a good number of SCs (Dev *et al.*, 2012a). De Coppi *et al.* (2007) reported that AF-derived cells have phenotypical characteristics of pluripotent SC, hence can differentiate into cells derived from different embryonic layers. It is easy to collect AF at the time of parturition as well as

during pregnancy through amniocentesis. The WJ is a gelatinous substance which is present in the umbilical cord (UC) where it surrounds the cord blood vessels. The WJ is composed of collagen fibers, proteoglycans and myofibroblasts stromal cells which can adhere to plastic and differentiate into many types of cells (Carlin *et al.*, 2006).

Buffalo is an important animal of South Asia and Europe as it provides milk, meat and traction power hence called Black Gold (Bilal *et al.*, 2006). Due to the importance of SCs in regenerative medicine and their transdifferentiation ability into many cell lines, they can be used to address many problems of buffalo. However, the importance lies in the fact of identifying cell isolation sites and further their differentiation properties.

There is a dearth of scientific literature on SCs derived from Nili-Ravi buffalo, specifically on bovine MSCs (bMSCs) derived from fetal adnexa; however, some studies reported the richness of AF and WJ with MSCs in humans (Widowati *et al.*, 2019) and bovines (Yadav *et al.*, 2011; Corradetti *et al.*, 2013). This study on fetal adnexa-derived MSCs from Nili-Ravi buffalo aimed to provide a deep insight into their characterization, proliferation and differentiation capabilities.

## MATERIALS AND METHODS

**Collection and transportation of samples:** For sampling of AF and WJ from Nili-Ravi buffalo, pregnant uteri (n=3) from the 2<sup>nd</sup> trimester were obtained from the slaughterhouse of Rawalpindi/Islamabad after approval from Institutional Biosafety and Bioethics Committee (IBC,1771/ORIC). The uteri were transported to Cell Culture Laboratory of Cytogenetics, PMAS-Arid Agriculture University, Rawalpindi, Pakistan, where they were disinfected with 70% isopropanol (Sigma, USA) and ethanol (Sigma, USA).

**Isolation, culturing and passaging of cells:** To collect AF-bMSCs, about 50mL of AF was aspirated and centrifuged at 400g for 10 minutes. After discarding the supernatant, pellet was incubated in defined media (DM) containing Dulbecco's Modified Eagle's Medium/Ham F-12 (DMEM/F-12), supplemented with 10% fetal bovine serum (FBS, Biowest, France), 1% antibiotics penicillin/streptomycin (100 units/mL and 100 ug/mL, respectively; Biowest, France), 1% amphotericin B (0.25 µg/mL, Biowest, France) at 37°C in the presence of 5% CO<sub>2</sub>.

The WJ samples were obtained in Dulbecco's phosphate-buffered saline (DPBS) without Ca<sup>2+</sup> and Mg<sup>2+</sup>. WJ was diced into pieces/ explants (~1-2 mm<sup>3</sup>) and digested with trypsin-EDTA (0.05% and 0.53mM, respectively) for half an hour and subsequently incubated with DM for five to seven days. Following confluence (~80%), bMSCs were trypsinized for passaging towards the next passage up to passage 2 (P2) which was used in subsequent experiments given below. Throughout the experiment, media was changed twice a week to keep the cells healthy.

**Growth kinetics:** Recovered bMSCs from P2 were seeded at a density of 5×10<sup>3</sup> cells per well in a 48-well cell

culture plate (Corning, USA), and growth kinetics were measured on days 3, 6, 9 and 12. After trypsinization, the population doubling time (PDT) was calculated with the following formula (Lu *et al.*, 2018):

$$PDT = \frac{\log_2(t - t_0)}{(\log N_t - \log N_0)}$$

Here PDT: population doubling time, t: harvesting time, t<sub>0</sub>: initial time, N<sub>t</sub>: harvested cell number, and N<sub>0</sub>: seeded cell number.

**Cell metabolic activity:** The extent of metabolism in recovered bMSCs was measured through 3-(4,5-Dimethylthiazol-2-yl)-2,5-diphenyltetrazolium bromide (MTT) assay. For this purpose, bMSCs (5×10<sup>3</sup> cells per well) were seeded in a 48-well cell culture plate. On every third day till day 12, bMSCs were treated with 150µL working solution (0.25 µg/mL) of MTT per well, incubated for 2.5h and formed formazan was eluted in 100µL of dimethyl sulfoxide (DMSO). Optical density (OD) analysis was performed at 630nm.

**In vitro mesodermal lineage differentiation assays:** Adipo- and osteogenic induction of bMSCs at P3 was carried out in a 24-well cell culture plate (Corning, USA) at a seeding density of 2.5×10<sup>4</sup> cells per well for confluence as described by Rashid *et al.*, (2021).

**A. Adipogenic induction:** Adipogenesis in bMSCs was induced in a two-step procedure; first induction (48 hours) and second maintenance (seven days). To induce adipogenesis, an induction media containing DMEM/F-12 supplemented with 10% FBS, 1% antibiotics, IBMX (0.1mM; Sigma, USA), rosiglitazone (10µM; BD Chemicals, Germiston, South-Africa), dexamethasone (0.3 mM; Solarbio, Shanghai, China) and 0.142% insulin (5 µg/ml; Nov, Denmark) was used. For maintenance, adipogenic maintenance media containing DMEM/F-12 supplemented with 1% Ex-cyte (Darmstadt, Germany), 0.142% insulin, 1% antibiotics were used. Subsequently, the cells were fixed with 4% buffered formalin (Sigma, USA), followed by oil red-O (ORO) staining at a concentration of 6:4 with distilled water and observed under the microscope. Then ORO elution was performed with absolute isopropanol and optical density (OD) of eluted stain was measured at 510nm.

The surface area occupied by ORO stain within a cell was estimated with the help of ImageJ software (1.50i, National Institutes of Health, USA) by processing individual cells at 8-bit. The total cellular area of adipocyte and ORO stained regions were determined using the "Threshold" function at "Auto" settings.

**B. Osteogenic induction:** For osteogenesis, bMSCs were incubated for 21 days in an osteogenic induction medium containing α-MEM (Gibco, USA) supplemented with 10% FBS, 1% antibiotics, β-glycerol phosphate (1µM; Sigma, USA), 0.01% dexamethasone (1 mM) and ascorbic acid (50 µM; Sigma, USA). Cells were fixed, followed by staining with Alizarin Red-S (ALZ), and observed for mineral deposition at 10x and 40x.

For quantification of ALZ, five areas (Fig. 4-I) per well were photomicrographed and analyzed by ImageJ using green channel under the “RGB stack” option at “Threshold” level 75. The measurements of highlighted areas were recorded as a percentage out of the total microscopic field (Booyesen *et al.*, 2018).

**Alkaline Phosphate (ALP) activity of osteogenesis:** To access the activity of ALP, bMSC were scratched from cell culture plates and analyzed through a commercially available kit (ELITech Group, France) according to the manufacturer instructions. The ALP concentration was measured by utilizing p-nitrophenyl phosphate as a substrate and normalized to the total protein present in the cell lysate.

**Immunocytochemistry (ICC):** To localize mesenchymal cell markers (CD73; ab137595 and CD90; ab92574), adipogenic specific marker (FABP4; ab85875) and osteogenic specific marker (osteopontin; ab63856) at P3, bMSCs were seeded at a density of  $1 \times 10^6$  cells per well in a 6-well cell culture plate preloaded with 6mm sterile coverslips. At the culmination of the induction period, the cells were fixed, treated with 0.3% triton (Triton® X-100), and blocked with goat serum (10%). Then the cells were incubated overnight with primary antibodies followed by incubation with secondary antibodies while nuclear identification was done by counterstaining with 2 µg/mL of DAPI (4',6-diamidino-2-phenylindole). The coverslips were mounted using an anti-bleach mounting medium (Vecta shield, St. Neots, UK) and were visualized under a fluoresce microscope.

**Fetal age estimation:** The curved-crown rump length (CVRL) measurement of the fetus was obtained for age determination (Soliman, 1975):

$$Y = 28.66 + 4.496(X) \quad \dots\dots\dots \text{(if CVRL is } < 20\text{cm)}$$

$$Y = 73.544 + 2.256(X) \quad \dots\dots\dots \text{(if CVRL is } \geq 20\text{cm)}$$

Here, Y is fetal age / gestational length in days and X is CVRL (cm).

**Statistical analysis:** Statistical analysis was performed using Minitab® 17.1.0 software. The experiments were conducted in duplicate while three replicates of each experiment parameters of growth kinetics and cell metabolic assay were performed and the results were expressed as mean  $\pm$  SEM. Data was analyzed by one-

way ANOVA for multiple mean comparisons using Tukey’s Honestly Significant test ( $P < 0.05$ ).

## RESULTS

The CVRL measurement of the fetus showed that average gestation length of samples was  $129 \pm 14.3$  days. On microscopic examination, fibroblast-like cells started to emerge from explants (Fig. 1b). The AF and WJ-bMSCs appeared similar at the confluence (Fig. 1a, c). The growth kinetics at P3 revealed that PDT was  $79.86 \pm 6.45$  and  $72.64 \pm 2.02$  hours, for AF and WJ-bMSCs, respectively. The growth curves, drawn from mean values of the number of bMSCs, showed a logarithmic trend, and no plateau phase was observed (Fig. 2a). However, AF-bMSCs exhibited a rapid increase in cell number from day 9 to 12. MTT assay showed that bMSCs have a high metabolic activity on days 3 and 6 which gradually decreased from day 9 to 12 (Fig. 2b).

**In vitro mesodermal differentiation:** After adipogenic induction for seven days, bMSCs from both the tissues were successfully differentiated into adipocytes, which was evident from rounded cell morphology and accumulation of lipid in the cytoplasm. The presence of intracytoplasmic lipid droplets was confirmed with ORO staining (Fig. 3-I). Control samples cultured in DM/control media did not show any change in cell morphology, while faint cytoplasmic/ membrane reactivity with ORO was observed in these cells. ORO concentration per cell of bMSCs induced groups was significantly ( $P < 0.05$ ) higher than their respective control groups, with the highest value in WJ-adipo-induced cells (Fig. 3-IIa). Significantly ( $P < 0.05$ ) higher ORO-stained surface area in adipo-induced bMSCs was recorded than their control groups, with the highest value in AF-adipo-induced bMSCs (Fig. 3-IIb). Immunopheno-typing expression of FABP4 was expressed successfully among adipo-induced cells of both the tissues (Fig. 5e, f). The presence of FABP4 accumulation was evident around the cell membrane as well as around unilocular and multilocular lipid droplets in adipose-induced bMSCs of both the tissues.

Under osteogenic induction, bMSCs differentiated into osteogenic lineage cells as they enlarged and modified their morphology contrary to control cells. Many osteogenic foci were observed which were formed by the accumulation of calcium or other minerals [hydroxylapatite mineral ( $\text{Ca}_{10}(\text{PO}_4)_6(\text{OH})_2$ )]. These minerals were

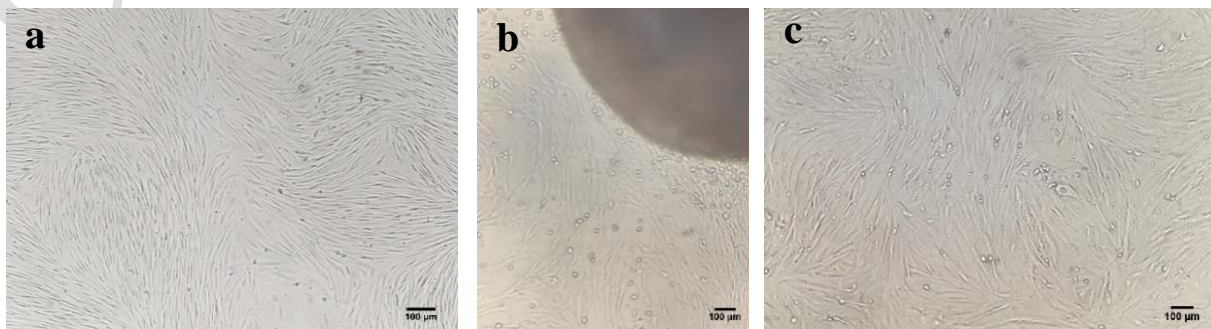


**Fig. 1.** Morphological features of AF-MSCs and WJ-MSCs in culture. AF-MSCs at the confluence of P2 (a), WJ explant is attached (day 5-7), and MSCs are migrating from it (b), WJ-MSCs at the confluence of P2 (c) in Nili-Ravi buffalo (*Bubalus bubalis*).

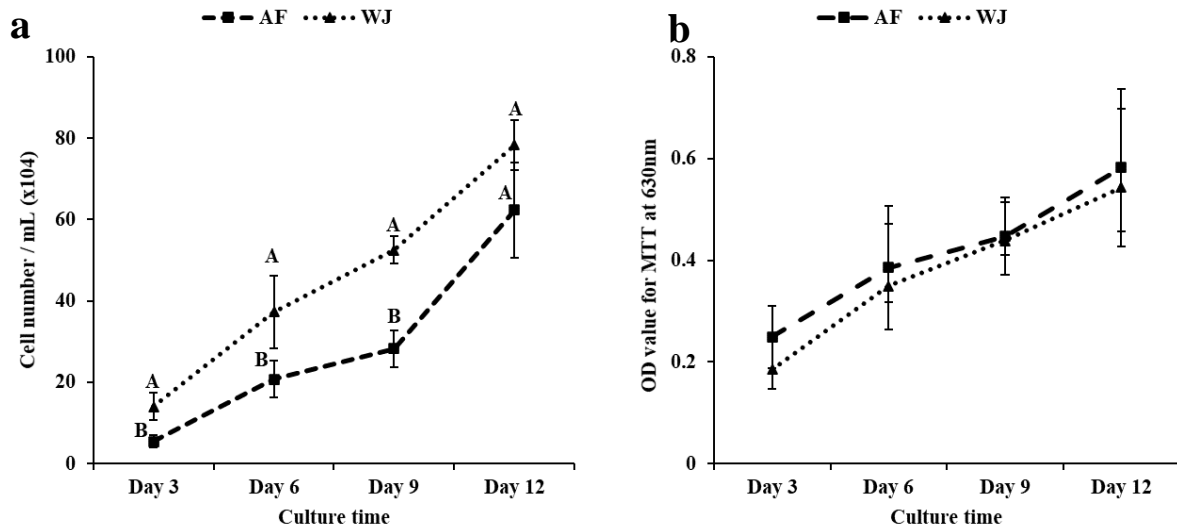


Fig. 2: Growth curve (a) and MTT absorbance value (b) of AF-MSCs and WJ-MSCs of Nili-Ravi buffalo (*Bubalus bubalis*) expressed as mean  $\pm$  SEM ( $P<0.05$ ).

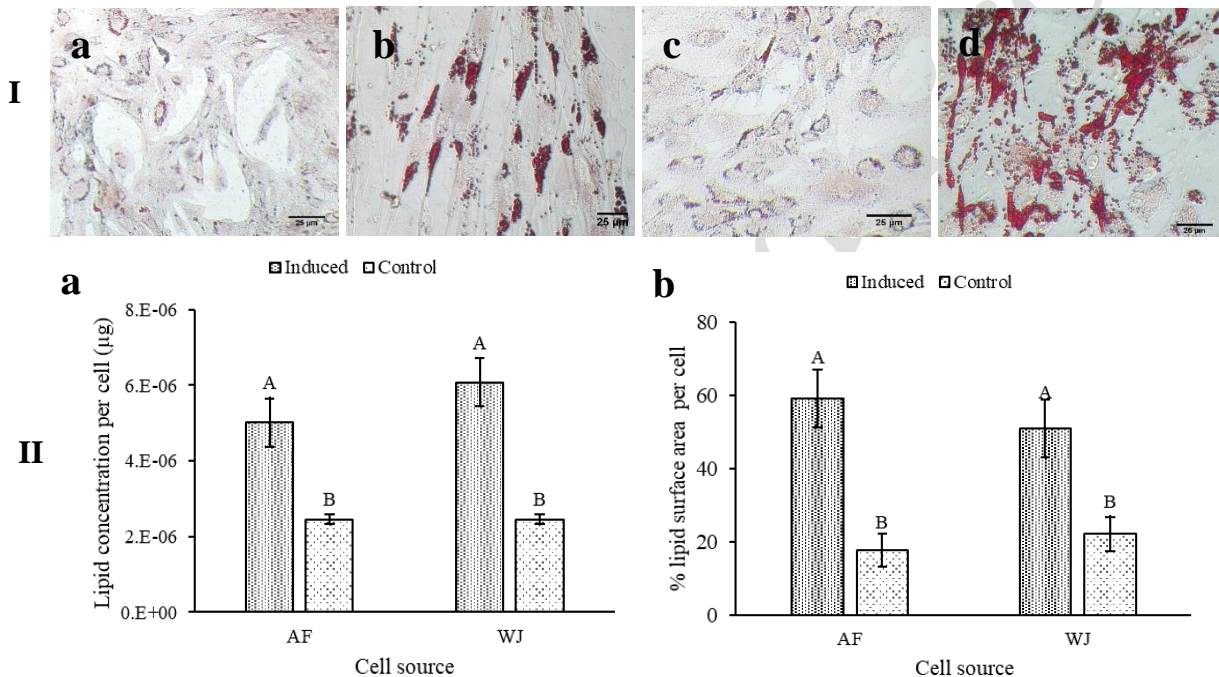
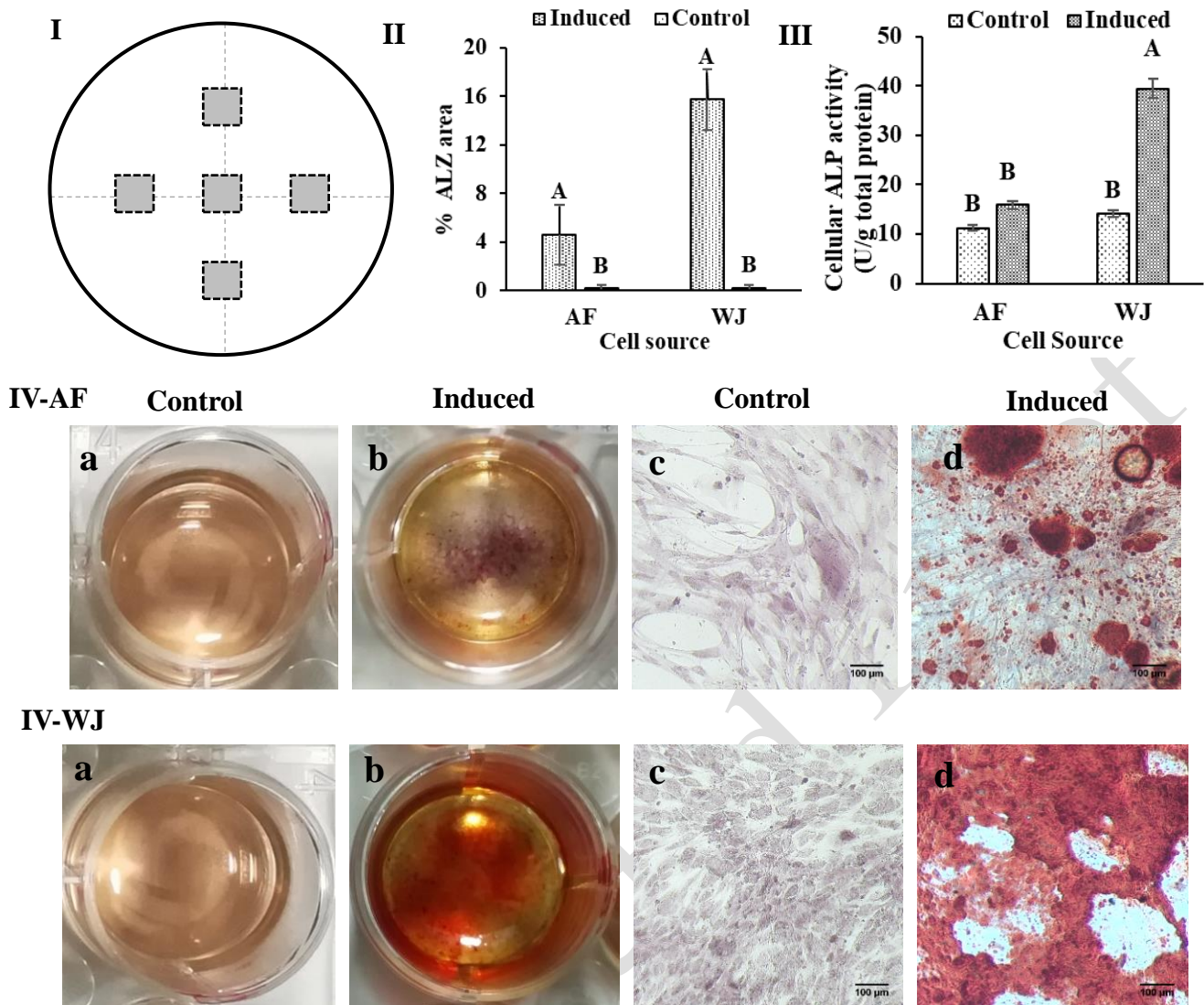


Fig. 3 (I-II): Adipogenic differentiation assay of AF and WJ-derived MSCs isolated from Nili-Ravi buffalo (*Bubalus bubalis*). (I) Intracytoplasmic lipid droplets appear red with ORO staining in induced AF (b) and WJ (d), while control AF (a) and WJ(c) did not show such cytoplasmic changes, only cell membrane lipids show light red color. (II) Lipid concentration per cell (a) and percent lipid surface area per cell (b) of each tissue, where A and B indicate a statistically significant difference ( $P<0.05$ ) between the control and induced groups.

secreted by the induced cells and appeared red by ALZ staining. Control cells cultured in DM did not show morphological changes and extracellular hydroxyl-apatite mineral deposits (Fig. 4-IV). ImageJ analysis of bMSCs of osteo-induced and control cells showed that AF and WJ induced cells had a very high extracellular calcium deposition, with WJ-oste-induced cells had remarkably high calcium deposits (Fig. 4-II) while in control groups, calcium deposition was scarce. ICC revealed the presence of osteopontin among osteo-induced cells of both the tissues (Fig.5g, h) and was uniformly distributed throughout the cytoplasm that confirms successful differentiation of bMSCs into the osteogenic lineage. Cellular ALP activity is considered an early marker of osteogenesis, which was assessed in the cellular lysate. The converted cells of both origins exhibited an increase of

ALP (U/g of protein) compared to control cells. However, WJ-derived bMSCs had significantly ( $P<0.05$ ) higher ALP activity as compared to AF-derived bMSCs (Fig. 4-III).

**Immunophenotyping:** An expression of mesenchymal cell surface markers is a characteristic parameter for detecting bMSCs which substantiates the evidence of the mesenchymal nature of cells. The ICC analysis exposed that bMSCs are positive for mesenchymal markers including CD73 and CD90 (Fig.5a-d). CD73 was localized near the nuclei, while CD90 was evenly distributed throughout the cell membrane. The intense presence of CD73 seems to be present in the Golgi apparatus and further has to be transported on the cell membrane. The results indicated that both sources provide cells that are similar to MSCs.



**Fig. 4 (I-IV):** *In vitro* differentiation assay of AF-MSCs and WJ-MSCs isolated from Nili-Ravi buffalo (*Bubalus bubalis*). (I) Schematic diagram of one well of a 24-well plate. The five small shaded squares on a cross represent the microscopic fields used for ALZ digital quantification. (II) ImageJ analysis of ALZ stained area out of the total microscopic field. Osteo-induced cells, specially WJ-MSCs, showed a massive degree of mineralization (mean±SEM) as compared to control, where a, b and c indicate a statistically significant difference ( $P<0.05$ ) between the control and induced groups. (III) ALP activity of bMSCs (mean±SEM) which was significantly ( $P<0.05$ ) the highest in induced WJ-bMSCs followed by induced AF-bMSCs. (IV) Positive staining of extracellular calcium/ mineral deposition with ALZ which indicates osteogenic lineage transdifferentiation (IV-AF & IV-WJ): b, d). Control cells maintained fibroblast morphology and stained negative with ALZ (IV-AF & IV-WJ): a, c).

## DISCUSSION

Fetal adnexa is a safe and readily available source of SCs as compared to conventional sources and is recognized as a highly potential source of bMSCs that yields an enormous number of cells in the subculture (Gugjoo *et al.*, 2019). During this trial at P0, AF showed a high number of non-adherent cells which were removed during media change, however, few rounded cells showed plastic adherence which was also reported in Holstein cow (Rossi *et al.*, 2014). Non-adherent cells having flat morphology come from the amniotic membrane, gastrointestinal, urogenital and respiratory epithelium (Dasgupta and Jain, 2016).

Unlike AF, WJ is a newer tissue to get attention as a source of bMSCs in human and veterinary science (Sree Kumar *et al.*, 2014), therefore, there is limited data available on growth kinetics and plasticity of WJ-bMSCs. For isolation of bMSCs from WJ two techniques viz,

explant attachment method and enzymatic digestion method are used. The former method provides a higher number of cells with higher expression of pluripotency markers while the latter method is easier and yields cells with a high proliferation rate and purity (Widowati *et al.*, 2019). In this study, both methods were combined to obtain the collective effect. Trypsin enzyme hydrolyzed the collagen fibers (Liu *et al.*, 2018) and released bMSCs. WJ-bMSCs were readily attached to plastic which is as per the principles established by the International Society of Cellular Therapy (ISCT) for the identification of MSCs (Dominici *et al.*, 2006). Like other reports (Corradetti *et al.*, 2014), our findings showed more than 90% viable cells; however, Vidane *et al.*, (2014) have reported less than 90% viability in feline. Uranio *et al.*, (2014) reported very low viability ( $71.40\pm 17.3\%$ ) in late passages (beyond P4) compared to early passages ( $92.83\pm 3.89\%$ ) in canines. Therefore, it is recommended to use MSCs at early passages to obtain maximum viable cells.

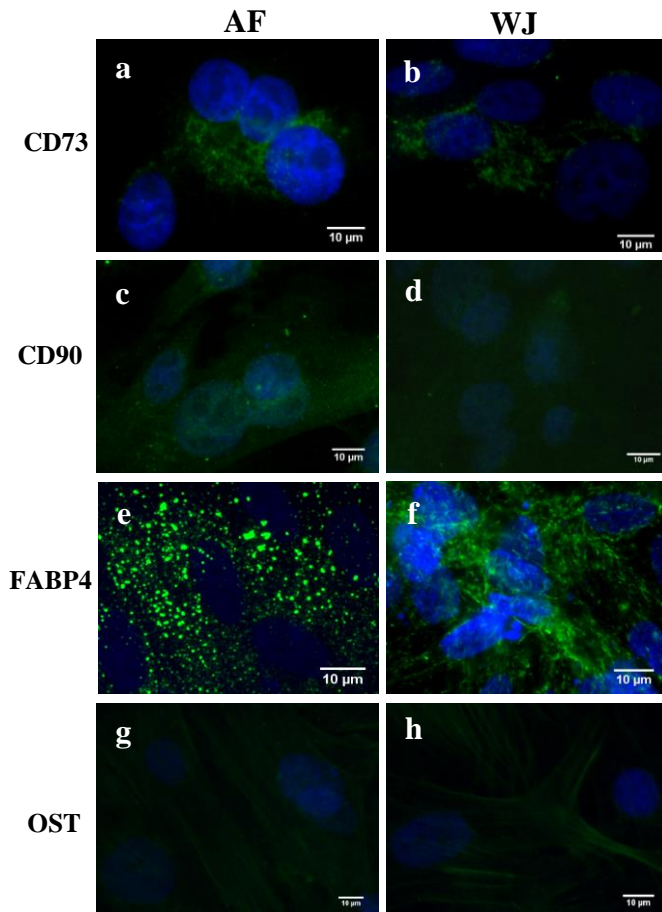


**Fig. 5:** Immunocytochemistry of AF-MSCs and WJ-MSCs isolated from Nili-Ravi buffalo (*Bubalus bubalis*). AF-MSCs and WJ-MSCs were labeled positively with immunofluorescence antibodies against mesenchymal specific markers including CD73 (a, b), CD90 (c, d). Adipogenic specific marker and osteogenic specific marker of both the cell types were labeled positively with immunofluorescence antibodies against FABP4 (e, f) and osteopontin (g, h). The presence of the cell was confirmed by nuclear counterstain with DAPI. Scale bar: 10 $\mu$ m.

The trajectory of the growth curve and population doubling time (PDT) are highly variable parameters among MSCs derived from different sources and at different stages of pregnancy. MSCs mostly showed a logarithmic growth pattern which is in line with our findings (Deng *et al.*, 2018). AF and WJ-bMSCs exhibited very high PDT (79.86 $\pm$ 6.45 and 72.64 $\pm$ 2.02 hours, respectively) which is comparable to that of AF-MSCs of Holstein cows (3.5 $\pm$ 1.6 days 84 $\pm$ 38.4 hours) (Rossi *et al.*, 2014) and feline (2.8 $\pm$ 3.2 days approximately 67.2 $\pm$ 76.8 hours) (Iacono *et al.*, 2012). However, it is higher than already recorded in buffalo amniotic membrane (60 $\pm$ 5 hours) (Deng *et al.*, 2018) and AF-MSCs of term pregnancy in cattle (2.69 $\pm$ 0.32 days approximately 64.56 $\pm$ 7.68 hours) (Corradetti *et al.*, 2013). The difference may be due to different types of tissues and stages of pregnancy.

An initial high metabolic activity was recorded in bMSCs that gradually decreased towards day 12. This finding is in agreement with the amniotic SC of rabbits where an initial wave of proliferation was recorded, followed by a drop in proliferation rate, which rebounded at the end of the experiment (Borghesi *et al.*, 2017). These findings are, however, contrary to data obtained from fibroblast cells of cat amniotic membrane (Vidane *et al.*,

2014) who reported continuous growth. This discrepancy may be due to their use of a fewer number of seeded cells per area. There is no data available to compare the results with bovines.

The bMSCs transdifferentiated into mesodermal adipogenic and osteogenic lineages which is evident from ORO and ALZ staining. Previously, fetal adnexa-derived MSCs in bovine (Deng *et al.*, 2018) and ovine (Lu *et al.*, 2018) have been transformed into these lineages. In this study, the cells were converted into adipocytes at the end of the experiment, however, the period of lipid concentration decreased from fourteen days (Jurek *et al.*, 2020) to seven days, which may be considered an achievement in the rapid conversion of bMSCs into functional adipocytes.

The lipid concentration measured in terms of OD value showed the highest concentration in WJ-adipo-induced cells while the image analysis method showed the highest concentration in AF-adipo-induced cells. This difference may be because the elution method measured the total lipid present in the cells, while ImageJ calculated ORO stained surface area. It can be seen that AF-adipo-induced cells were more flattened and occupied a greater surface area than that of WJ-adipo-induced cells which were relatively spherical. This inconsistency can be resolved by using 3D scanning electron microscopic (SEM) images of both cell types.

Osteogenesis was observed in induced AF-bMSCs by ALZ staining which is at par with previously reported findings in bovines (Jurek *et al.*, 2020). Similarly, induced WJ-bMSCs were also confirmed for osteogenic lineage differentiation which has also been reported in adipose-derived bMSCs (Sreekumar *et al.*, 2014). ALZ quantification (Booyesen *et al.*, 2018) of stained cells revealed that a very high concentration of extracellular hydroxyl-apatite mineral was secreted by WJ-bMSCs suggesting that they possess higher osteogenic differentiation potential than AF-bMSCs (Conconi *et al.*, 2011).

The FABP4, which is considered as an intermediate and late maker of adipogenic differentiation assay, was also detected in both bMSCs which is in agreement with previous findings in human AF-MSCs (Conconi *et al.*, 2011) and bovine AF-MSCs (Sandhu *et al.*, 2017; Jurek *et al.*, 2020). Similarly, in this study osteogenic specific gene (osteopontin) was identified in both induced cells, AF- and WJ-bMSCs, which was also reported in cattle-AF (Rossi *et al.*, 2014). As MSCs must express a positive reaction for mesenchymal-specific genes (Dominici *et al.*, 2006), the results of immunofluorescence suggested that AF- and WJ-bMSCs had a positive expression of these mesenchymal markers.

**Conclusions:** It may be inferred that cells derived from AF and WJ of Nili-Ravi buffalo during second-trimester pregnancy are similar to MSCs by their phenotypic characteristics, *in vitro* differentiation ability, renewability and plastic adherence, however, WJ-bMSCs exhibited better differentiation potential than AF-bMSCs.

**Authors contribution:** This manuscript is from the Ph.D. thesis of AS. ASQ and MAS conceived the idea and designed the study. AS conducted the experiments. All

authors were involved in data interpretation, write-up, and final approval of the manuscript. We, the authors declare no financial/ intellectual conflict of interest with any person/ company or institution.

**Acknowledgments:** This piece of research work was financially supported by HEC Ph.D. Indigenous Scholarship (PIN#417-30654-2VS4-008).

## REFERENCES

- Bilal MQ, Suleman M and Raziq A, 2006. Buffalo: Black gold of Pakistan. *Livest Res Rural Dev* 18:128.
- Booyesen E, Gijssen HS, Deane SM, et al., 2018. The effect of vancomycin on the viability and osteogenic potential of bone-derived mesenchymal stem cells. *Probiotics Antimicrob Proteins* 11:3-8.
- Borghesi J, Mario LC, Carreira ACO, et al., 2017. Phenotype and multipotency of rabbit (*Oryctolagus cuniculus*) amniotic stem cells. *Stem Cell Res Ther* 8:1-14.
- Campos LL, Landim-Alvarenga FC, Ikeda TL, et al., 2017. Isolation, culture, characterization and cryopreservation of stem cells derived from amniotic mesenchymal layer and umbilical cord tissue of bovine fetuses. *Pesqui Vet Bras* 37:278-86.
- Carlin R, Davis D, Weiss M, et al., 2006. Expression of early transcription factors Oct-4, Sox-2 and Nanog by porcine umbilical cord (PUC) matrix cells. *Reprod Biol Endocrinol* 4:8-21.
- Conconi MT, Liddo R Di, Tommasini M, et al., 2011. Phenotype and differentiation potential of stromal populations obtained from various zones of human umbilical cord: An overview. *Open Tissue Eng Regen Med J* 4:6-20.
- Corradetti B, Meucci A, Bizzaro D, et al., 2013. Mesenchymal stem cells from amnion and amniotic fluid in the bovine. *Reproduction* 145:391-400.
- Corradetti B, Correani A, Romaldini A, et al., 2014. Amniotic membrane-derived mesenchymal cells and their conditioned media: Potential candidates for uterine regenerative therapy in the horse. *PLoS One* 9:1-9.
- Dasgupta S and Jain SK, 2016. Importance of amniotic fluid in gastrointestinal development. *NeoReviews* 17:e367-e76.
- De Coppi P, Bartsch G, Siddiqui MM, et al., 2007. Isolation of amniotic stem cell lines with potential for therapy. *Nat Biotechnol* 25:100-6.
- de Moraes CN, Maia L, de Oliveira E, et al., 2017. Shotgun proteomic analysis of the secretome of bovine endometrial mesenchymal progenitor/ stem cells challenged or not with bacterial lipopolysaccharide. *Vet Immunol Immunopathol* 187:42-7.
- Deng Y, Huang G, Zou L, et al., 2018. Isolation and characterization of buffalo (*Bubalus bubalis*) amniotic mesenchymal stem cells derived from amnion from the first trimester pregnancy. *J Vet Sci* 80:710-9.
- Dev K, Gautam SK, Giri SK, et al., 2012. Isolation, culturing and characterization of feeder-independent amniotic fluid stem cells in buffalo (*Bubalus bubalis*). *Res Vet Sci* 93:743-8.
- Dominici M, Blanc K Le, Mueller I, et al., 2006. Minimal criteria for defining multipotent mesenchymal stromal cells. The International Society for Cellular Therapy position statement. *Cytotherapy* 8:315-7.
- Gugjoo MB, Amarpal, Fazili MR, et al., 2019. Mesenchymal stem cell: Basic research and potential applications in cattle and buffalo. *J Cell Physiol* 234:8618-35.
- Iacono E, Cunto M, Zambelli D et al., 2012. Could fetal fluid and membranes be an alternative source for Mesenchymal Stem Cells (MSCs) in the feline species? A preliminary study. *Vet Res Commun* 36:107-118.
- Jurek S, Sandhu MA, Trappe S, et al., 2020. Optimizing adipogenic transdifferentiation of bovine mesenchymal stem cells: a prominent role of ascorbic acid in FABP4 induction. *Adipocyte* 9:35-50.
- Kumar D, Anand T, Lalaji SN, et al., 2015. Buffalo embryonic, fetal and adult stem cells: progress and challenges. *Agric Res* 4:7-20.
- Liu ZQ, Tuo FY, Song L, et al., 2018. Action of trypsin on structural changes of collagen fibres from sea cucumber (*Stichopus japonicus*). *Food Chem* 256:113-8.
- Lu T, Pei W, Zhang S, et al., 2018. *In vitro* culture and biological characteristics of sheep amniotic mesenchymal stem cells. *Pak J Zool* 50:1629-38.
- Rashid U, Sandhu MA, Yaqoob M et al., 2021. Critical bone gap repair using autologous adipose derived canine mesenchymal stem cell graft. *Pak Vet J*. DOI: 10.29261/pakvetj/2021.050
- Rossi B, Merlo B, Colleoni S, et al., 2014. Isolation and *in vitro* characterization of bovine amniotic fluid derived stem cells at different trimesters of pregnancy. *Stem Cell Rev Rep* 10:712-24.
- Sandhu MA, Jurek S, Trappe S, et al., 2017. Influence of bovine serum lipids and fetal bovine serum on the expression of cell surface markers in cultured bovine preadipocytes. *Cells Tissues Organs* 204:13-24.
- Soliman M, 1975. Studies on the physiological chemistry of the allantoic and amniotic fluids of buffaloes at the various periods of pregnancy. *Indian Vet J* 52:106-12.
- Sreekumar T, Ansari MM, Chandra V, et al., 2014. Isolation and characterization of buffalo Wharton's jelly derived mesenchymal stem cell. *Stem Cell Res Ther* 4:207.
- Uranio MF, Dell'acqua ME, Caira M, et al., 2014. Characterization and *in vitro* differentiation potency of early-passage canine amnion- and umbilical cord-derived mesenchymal stem cells as related to gestational age. *Mol Reprod Dev* 81:539-51.
- Vidane AS, Souza AF, Sampaio RV, et al., 2014. Cat amniotic membrane multipotent cells are nontumorigenic and are safe for use in cell transplantation. *Stem Cells and Cloning: Adv Appl* 7:71-8.
- Widowati W, Gunanegara RF, Rizal R, et al., 2019. Comparative analysis of Wharton's jelly mesenchymal stem cell (WJ-MSCs) isolated using explant and enzymatic methods. In: *The 1st International Seminar on Smart Molecule of Natural Resources*. Journal of Physics: Conference Series, IOP Publishing, UK, p: 012024.
- Yadav PS, Mann A, Singh V, et al., 2011. Expression of pluripotency genes in buffalo (*Bubalus bubalis*) amniotic fluid cells. *Reprod Domest Anim* 46: 705-11.